BIOCHEMISTRY
including biophysical chemistry & molecular biology
Article

Biochemistry **2010,** *49,* 5753–5759 5753
DOI: 10.1021/bi1002376

From Gene Delivery to Gene Silencing: Plasmid DNA-Transfecting Cationic Lipid 1,3-Dimyristoylamidopropane-2-[bis(2-dimethylaminoethane)] Carbamate Efficiently Promotes Small Interfering RNA-Induced RNA Interference[†]

Michael Spelios, Molinda Kearns, and Michalakis Savva*

Division of Pharmaceutical Sciences, Arnold and Marie Schwartz College of Pharmacy and Health Sciences, Long Island University, Brooklyn, New York 11201

Received February 16, 2010; Revised Manuscript Received May 28, 2010

ABSTRACT: The cationic lipid 1,3-dimyristoylamidopropane-2-[bis(2-dimethylaminoethane)] carbamate (1,3lb2) was applied as a delivery system for small interfering RNA (siRNA) to inhibit the production of vascular endothelial growth factor (VEGF) in vitro in human prostate carcinoma cell line PC-3. VEGF protein silencing peaked at 94% when cationic lipid−nucleic acid complexes (lipoplexes) were formulated at a nitrogen:phosphorothioate ratio (N:P) of 2 with a dose concentration of 53.7 nM, and the performance of these lipoplexes was not impeded by serum. Knockdown efficiency was maintained for at least 72 h, and an IC_{50} of 12 nM lasted for 48 h. Only 20% of the total siRNA became cell-associated at this N:P, at a rate of 25 ng/h. Lipoplexes of the optimal formulation were relatively monodisperse, having an average diameter of 634 nm and a ζ potential of −21.3 mV. Formation of the 1,3lb2−siRNA complex reached 94% at an N:P of 2 and was positively cooperative; the binding constant was calculated in the range of 10^5 M^{-1}, and a Hill coefficient of 3 was determined. 1,3lb2 was found to be a nontoxic and potent carrier of siRNA that binds to the nucleic acid effectively and whose lipoplexes promote long-lasting inhibition, have high biological activity at low N:Ps, and are functional in the presence of serum.

RNA interference (RNAi)[1] was first described by the Nobel Prize-winning work of Fire and co-workers (*1*) more than a decade ago in the nematode *Caenorhabditis elegans*, followed three years later by its first description in mammalian cells (*2*). RNAi is an evolutionarily conserved defense mechanism against viruses and transposons (*3*). This naturally occurring process is triggered by duplex RNAs that induce enzymatic degradation of complementary mRNA, resulting in sequence-specific knockdown of gene expression.

Since its role in normal gene silencing was ascertained, RNAi quickly became a popular tool for functional genomics and has been used in numerous therapeutic applications for the downregulation of disease-causing genes in ocular diseases, neurodegenerative disorders, viral infections, and cancers (*4*, *5*). Synthetic double-stranded small interfering RNAs (siRNAs) were developed to harness the RNAi pathway that is innately guided by endogenous molecules known as micro RNAs. One such siRNA targeting vascular endothelial growth factor (VEGF) was constructed as a cancer therapeutic (*6*). VEGF is a secreted protein involved in angiogenesis and has been linked to tumor growth and metastasis (*7*−*9*).

When potential siRNA transporters are being sought, it is only logical to first investigate those with proven efficacy in transfecting plasmid DNA (pDNA) and antisense oligonucleotides. Among these possibilities, cationic liposome/lipid-mediated siRNA cellular delivery (siFection) (*10*) holds tremendous promise. The cationic lipid 1,3-dimyristoylamidopropane-2-[bis(2-dimethylaminoethane)] carbamate, henceforth termed 1,3lb2 (Scheme 1), is an established delivery system for pDNA; the biological activity and physicochemical properties of 1,3lb2, alone and in cationic lipid−nucleic acid complexes (lipoplexes) with pDNA, are detailed elsewhere (*11*, *12*). In this work, 1,3lb2 was studied as a carrier of siRNA for the suppression of VEGF production in vitro in human prostate carcinoma cell line PC-3.

EXPERIMENTAL PROCEDURES

Materials. VEGF-siRNA and scrambled (scr) siRNA sequences, the latter serving as a nonsilencing control, were taken from Takei et al. (*6*) and synthesized by Qiagen (Valencia, CA), but modified with two thiolated strands to prevent hydrolysis of the ribonucleic acid (Scheme 2). Fluorescein isothiocyanate (FITC)-labeled siRNA was also from Qiagen, with the FITC tag covalently linked to the 5′-end of the sense strand. All siRNAs were purified by denatured ion-exchange high-performance liquid chromatography (HPLC) and native reversed-phase HPLC, and the sequence and identity of each duplex were confirmed by matrix-assisted laser desorption ionization time-of-flight mass spectrometry. The siRNAs were supplied as powders and stored at −20 °C; prior to use, they were reconstituted to a concentration of 1 mg/mL in RNase-free TE buffer (pH 8). 1,3lb2

[†]This work was supported in part by a Predoctoral Fellowship in Pharmaceutics from the PhRMA Foundation (Washington, DC) and by National Institutes of Health Grant EB004863.

*To whom correspondence should be addressed. Phone: (718) 488-1471. Fax: (718) 780-4586. E-mail: msavva@liu.edu.

[1]Abbreviations: 1,3lb2, 1,3-dimyristoylamidopropane-2-[bis(2-dimethylaminoethane)] carbamate; ELISA, enzyme-linked immunosorbent assay; EtBr, ethidium bromide; FBS, fetal bovine serum; FITC, fluorescein isothiocyanate; HPLC, high-performance liquid chromatography; lipoplex, cationic lipid−nucleic acid complex; MTT, 3-(4,5-dimethylthiazol-2-yl)-2,5-diphenyltetrazolium bromide; N:P, nitrogen:phosphorothioate ratio; PDI, polydispersity index; pDNA, plasmid DNA; PEC, polyelectrolyte complex; RNAi, RNA interference; RT-PCR, reverse transcription polymerase chain reaction; scr, scrambled; SFM, serum-free medium; siFection, cationic liposome/lipid-mediated siRNA cellular delivery; siRNA, small interfering RNA; VEGF, vascular endothelial growth factor; WSLP, water-soluble lipopolymer.

Published on Web 06/02/2010

was synthesized and identified to purity (>99%) as previously described (*12*). All other reagents and solvents were purchased from commercial vendors and used without further purification.

Methods. (*i*) *Cell Culture*. PC-3 cells (American Type Culture Collection, Manassas, VA) in F-12K Medium supplemented with 10% fetal bovine serum (FBS) were maintained at 37 °C in a 5% CO_2 in air humidified atmosphere. The day before siFection, cells were seeded at the desired number in multiwell plates and left overnight to attach.

(*ii*) *Cationic Lipid Dispersion and Lipoplex Preparation*. A solution of 1,3lb2 in chloroform was dried under a stream of nitrogen gas followed by high-vacuum desiccation. The dry lipid film was resuspended in 40 mM Tris (pH 7.2), at an elevated temperature with periodic vortexing, for a final concentration of 0.3 mM 1,3lb2. Lipoplexes were formed at various nitrogen: phosphorothioate ratios (N:Ps) in serum-free F-12K Medium (SFM) by pipetting an aliquot of siRNA solution into an appropriate dilution of lipid dispersion.

(*iii*) *SiFection Studies*.

(*a*) *Bioactivity*. Lipoplexes were incubated with cells (300000 cells/well, 12-well plate) for 3 h. Then lipoplexes were replaced with fresh serum medium, and cells were incubated for the desired length of time. For serum studies, 250 μL of lipoplexes was diluted within the wells in an equal volume of serum medium to give a final FBS concentration of 5%. A standard 3-(4,5-dimethylthiazol-2-yl)-2,5-diphenyltetrazolium bromide (MTT) assay was used to evaluate cytotoxicity.

VEGF protein was quantified from the cell medium using an immunoassay kit (Invitrogen, Camarillo, CA) according to the manufacturer's instructions. Inhibition of protein production was calculated by

$$\% \text{ knockdown} = \frac{[\text{VEGF}]_{\text{untreated}} - [\text{VEGF}]_{\text{treated}}}{[\text{VEGF}]_{\text{untreated}}} \times 100 \quad (1)$$

where $[\text{VEGF}]_{\text{untreated}}$ and $[\text{VEGF}]_{\text{treated}}$ are concentrations of protein from untreated cells and cells treated with lipoplexes, respectively.

Scheme 1: Molecular Structure of 1,3lb2

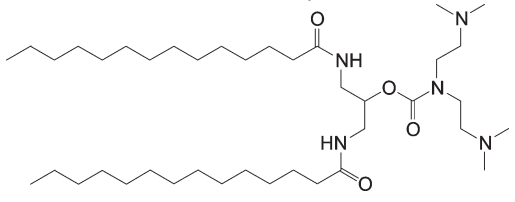

Scheme 2: VEGF-siRNA and Scrambled siRNA Sequences[a]

VEGF-siRNA

Sense: 5' r(psG-psG-psA-psG-psU-psA-psC-psC-psC-psU-psG-psA-psU-psG-psA-psG-psA-psU-psC) d(TT) 3'

Antisense: 3' d(TT) r(psC-psC-psU-psC-psA-psU-psG-psG-psG-psA-psC-psU-psA-psC-psU-psC-psU-psA-psG) 5'

Scr-siRNA

Sense: 5' r(psA-psC-psG-psC-psG-psU-psA-psA-psC-psG-psC-psG-psG-psG-psA-psA-psU-psU-psU) d(TT) 3'

Antisense: 3' d(TT) r(psU-psG-psC-psG-psC-psA-psU-psU-psG-psC-psG-psC-psC-psC-psU-psU-psA-psA-psA) 5'

[a]The backbone phosphates were substituted for phosphorothioate groups, symbolized by ps.

VEGF mRNA was quantified from cell lysates by real-time reverse-transcription polymerase chain reaction (RT-PCR) using a 7300 Real-Time PCR System (Applied Biosystems, Foster City, CA), Qiagen's QuantiTect SYBR Green RT-PCR Kit, and validated VEGF and β-actin (internal control) primer sets also from Qiagen. Total RNA was purified from cells using Qiagen's RNeasy Plus Mini Kit. The real-time cycler conditions were as follows: one cycle of reverse transcription at 50 °C for 15 min, PCR initialization at 95 °C for 15 min, 40 cycles of denaturation at 95 °C for 15 s, annealing at 60 °C for 1 min, and extension at 72 °C for 30 s. Expression levels of β-actin were identical in untreated and treated cells (not shown). Inhibition of VEGF mRNA production was calculated by eq 1.

(*b*) *Cellular Association*. SiFection was conducted with lipoplexes composed of FITC-labeled siRNA (0.5 μg/well, 67.1 nM). Lipoplexes were removed at half-hour intervals, and cells were lysed with a 0.1% Triton X-100 solution. Cell lysates were diluted in Tris buffer containing 0.1% SDS and analyzed for siRNA content at a λ_{ex} of 495 nm using a Cary Eclipse fluorescence spectrophotometer (Varian Australia Pty Ltd., Victoria, Australia). 1,3lb2 caused a shift in the FITC-siRNA emission peak to a longer wavelength and a lower intensity. Upon addition of SDS, the peak was restored to its original wavelength and intensity via decomplexation of the lipoplexes (Figure S1 of the Supporting Information). The peak fluorescence emission intensity of each sample was measured around 521 nm and converted to FITC-siRNA concentration from a standard curve (Figure S2 of the Supporting Information).

(*iv*) *Particle Size and* ζ *Potential Measurements*. Particle sizes and ζ potentials of lipoplexes were measured with a Zetasizer Nano ZS System (Malvern Instruments Ltd., Worcestershire, U.K.) as described by Spelios and Savva (*12*).

(*v*) *Complexation Studies*.

(*a*) *Fluorescence Titration*. In a quartz cuvette, ethidium bromide (EtBr) and siRNA (444 nM) were combined in SFM at a nucleotide:dye molar ratio of 44:1. At this ratio, the EtBr fluorescence emission intensity fell within the initial steep linear region of the intensity versus siRNA concentration plot (Figure S3 of the Supporting Information). Aliquots of lipid dispersion were added under constant stirring, and the peak intensity I around 600 nm was monitored spectrofluorometrically at a λ_{ex} of 510 nm. The extent of lipid−siRNA complexation was assessed from

$$\% \text{ binding} = \left(1 - \frac{I - I_{\text{blank}}}{I_0 - I_{\text{blank}}}\right) \times 100 \quad (2)$$

where I_{blank} is the intensity of an EtBr blank solution and I_0 is the intensity of EtBr in the presence of siRNA prior to the addition of

lipid. The % binding (y) was plotted as a function of N:P, and a sigmoidal equation of the form

$$y = A + \frac{B}{1 + e^{C(D-x)}} \quad (3)$$

was fit to the plot with PSI-Plot (version 7.01, Poly Software International, Inc., Pearl River, NY) through minimization of the sum of the squared residuals with four adjustable parameters at a 5% tolerance level. A and B are y_{max} and $y_{max} - y_{min}$, respectively; C is a shape parameter, and D is the N:P corresponding to 50% binding.

(b) Hill and Scatchard Analyses. Cationic lipid association with siRNA was studied using an infinite cooperativity model and an independent ligand model. For a siRNA molecule S with n binding sites of equal affinity exhibiting cooperative binding, the binding of lipid L to S can be described by the following equilibria where K_{A_i} is the respective association constant ($1 \leq i \leq n$):

$$L + S \leftrightarrow LS \quad K_{A_1} \quad (4)$$

$$L + LS \leftrightarrow L_2S \quad K_{A_2} \quad (5)$$

$$\vdots$$

$$L + L_{n-2}S \leftrightarrow L_{n-1}S \quad K_{A_{n-1}} \quad (6)$$

$$L + L_{n-1}S \leftrightarrow L_nS \quad K_{A_n} \quad (7)$$

The overall equation and the corresponding association constant are

$$nL + S \leftrightarrow L_nS \quad K = K_{A_1} \times K_{A_2} \ldots \times K_{A_{n-1}} \times K_{A_n} = {K_A}^n \quad (8)$$

$${K_A}^n = \frac{[L_nS]}{[L]^n[S]} \quad (9)$$

Bound and unbound fractions F_B and F_U, respectively, of S are

$$F_B = \frac{[L_nS]}{[S] + [L_nS]} \quad (10)$$

$$F_U = \frac{[S]}{[S] + [L_nS]} \quad (11)$$

Dividing eq 10 by eq 11 and substituting eq 9 for $[L_nS]$ give

$$\frac{F_B}{F_U} = \frac{[L_nS]}{[S]} = {K_A}^n[L]^n \quad (12)$$

Taking the logarithm of eq 12 gives the Hill equation:

$$\log \frac{F_B}{F_U} = n \log K_A + n \log[L] \quad (13)$$

Because F_B and F_U are ascertained from ΔI ($I_0 - I$) and I, respectively, $\log(\Delta I/I)$ (blank-corrected intensities) was plotted versus log[1,3lb2] to yield the Hill plot; n and K_A were obtained from the slope and intercept, respectively. The free lipid concentration was determined as described by Boger and co-workers (*13*).

Noncooperative cationic lipid binding on siRNA was studied using the well-known Scatchard equation:

$$\frac{F_B}{[L]} = nK_A - K_A F_B \quad (14)$$

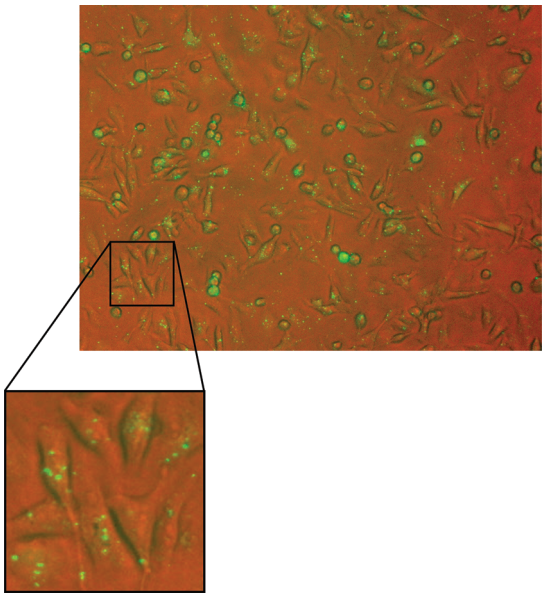

FIGURE 1: Representative image of cell-associated 1,3lb2−siRNA complexes. siRNA is seen by the fluorescence (green) of its FITC tag. The image was captured using an Axiovert 200M inverted microscope (Carl Zeiss, Göttingen, Germany).

(*c*) *Agarose Gel Electrophoresis*. Electrophoresis of lipoplexes was conducted on a 2% agarose gel with 0.2 μg of siRNA per well using a Horizon 58 Horizontal Gel Electrophoresis System (Life Technologies, Gibco BRL, Gaithersburg, MD). EtBr (0.5 μg/mL) was added to the gel and electrophoresis buffer (TAE, pH 7.4) for visualization of siRNA via a Gel Logic 200 Imaging System (Scientific Imaging Systems, Eastman Kodak Co., Rochester, NY). Band intensities were extracted with the Kodak 1D Image Analysis Software (version 3.6.3) and used to compute the % intensity decrease in each lane relative to the control (siRNA alone).

RESULTS AND DISCUSSION

SiFection Studies. (*i*) *Bioactivity*. Interaction between siRNA-containing lipoplexes and the cell surface is essential for transportation of the polyanionic duplex across the similarly negatively charged plasma membrane, and 1,3lb2 mediates this interaction very well. Figure 1 shows the strong association between 1,3lb2−siRNA complexes and PC-3 cells. The amount of siRNA in the lipoplexes (N:P of 2) was varied to examine the dose dependence of gene silencing. Cell media were collected post-siFection at 24 h intervals up to 72 h for VEGF quantification by an enzyme-linked immunosorbent assay (ELISA). Greater than 50% knockdown was observed at concentrations beyond 16.8 nM siRNA, and the level of knockdown at these concentrations was relatively stable over 3 days (Figure 2A). Further examination revealed an optimal dose concentration of 53.7 nM (0.4 μg/well) above which the knockdown remained constant at 90% (Figure 2B). The sequence specificity of siRNA-induced RNAi was verified by the absence of knockdown when scr-siRNA was used. No cytotoxicity was detected for any formulation.

The dose−response plots (Figure 2A) were curve-fitted with PSI-Plot using

$$y = \frac{100}{1 + \left(\frac{IC_{50}}{x}\right)^{slope}} \quad (15)$$

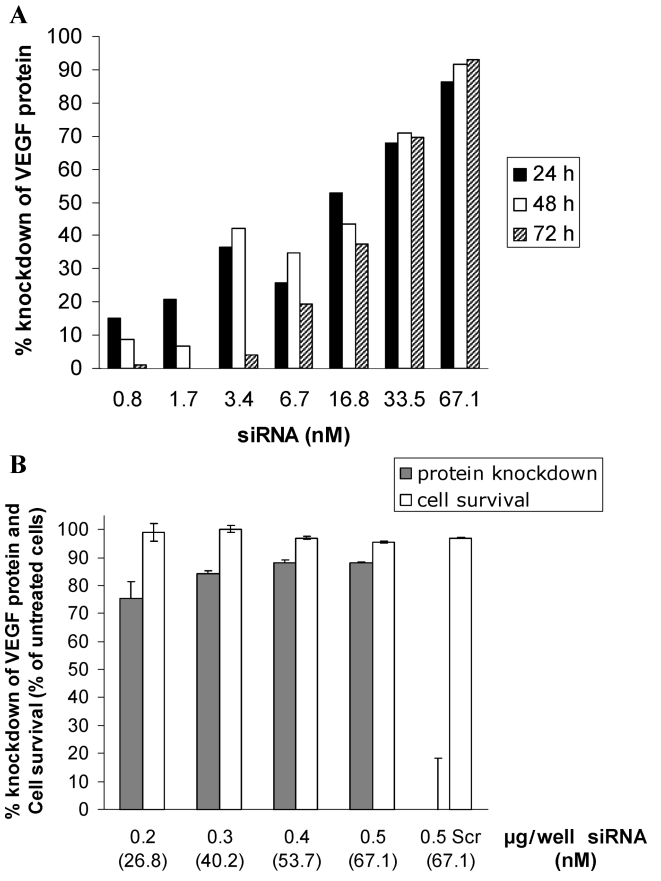

FIGURE 2: (A and B) Knockdown of VEGF protein (as determined by an ELISA) secreted into the media of PC-3 cells exposed to lipoplexes (N:P of 2) at various doses. (B) An ELISA and a MTT cytotoxicity assay were performed 48 h post-siFection. scr-siRNA served as a control. The results are expressed as the mean ± the standard deviation (n = 2).

where y is the % knockdown of VEGF protein, x is the siRNA concentration (nanomolar), IC_{50} is the dose concentration producing exactly 50% knockdown, and the slope is a shape parameter. IC_{50} was found to be 12 nM at 24 and 48 h, almost doubling to a value of 20 nM at 72 h (Table 1). The slope also nearly doubled from 0.75 and 0.87 at 24 and 48 h, respectively, to 1.7 at 72 h. Additionally, the fits at 24 and 48 h were hyperbolic, whereas the fit at 72 h was sigmoidal (not shown). From the data analysis, it appears that the inhibitory effect was reduced after 3 days. Most probably, at small doses, the constituents of the RNAi pathway were incompletely activated and the cells recovered within the tested time frame to resume normal VEGF production. Thus, knockdown at these doses was not as pronounced 3 days post-siFection as it was after 1−2 days, resulting in a lag at early points in the dose−response plot at 72 h which shifted the IC_{50} to a larger dose.

Subsequently, the N:P was optimized at the optimum dose. At an N:P of 0.5, there was no knockdown of VEGF protein, while lipoplexes at an N:P of 1 produced 86% knockdown (Figure 3A). Knockdown reached a maximum of 94% at an N:P of 2 and was maintained at higher N:Ps. No significant knockdown was seen with naked siRNA or lipoplexes incorporating scr-siRNA (not shown).

To confirm that protein knockdown was due to targeted degradation of corresponding mRNA, real-time RT-PCR was performed on cell lysates to quantitate VEGF mRNA. As shown in Figure 3A, the mRNA and its encoded protein were knocked down similarly.

Table 1: Curve-Fit Parameters of Dose−Response Plots (Figure 2A)

time post-siFection (h)	IC_{50} (nM)	slope	COD[a]
24	12.2	0.75	0.919
48	12.3	0.87	0.883
72	20.3	1.7	0.989

[a]Coefficient of determination.

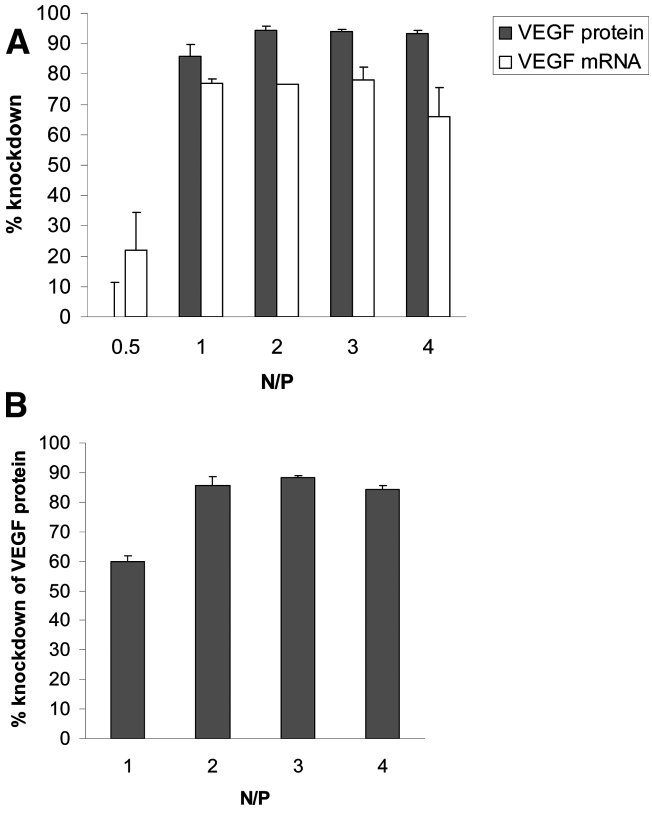

FIGURE 3: Effect of the N:P on the % VEGF knockdown (A) under serum-free conditions and (B) in the presence of 5% FBS. Experiments were conducted with 0.4 µg of siRNA/well (53.7 nM). Samples were collected 48 h post-siFection. The results are expressed as the mean ± the standard deviation (n = 2).

The influence of serum on 1,3lb2-mediated siFection was also examined. Serum had no effect on VEGF protein knockdown except at an N:P of 1 where the knockdown dropped from 86% under serum-free conditions to 60% in the presence of 5% FBS (Figure 3B).

(*ii*) *Cellular Association*. The kinetics of cellular association of 1,3lb2-complexed siRNA during siFection were studied. At an N:P of 0.5, the amount of cell-associated siRNA did not vary with time after 0.5 h (Figure 4 and Table 2). At an N:P of 1, there was a linear increase in the rate of cellular association (18 ng/h) from 0.5 until 1.5 h when the amount plateaued between 50 and 60 ng, twice the amount observed at an N:P of 0.5. It appears that at an N:P of 1 all excess free lipid not electrostatically complexed with siRNA was exhausted after 1.5 h. At an N:P of 0.5, depletion of excess lipid occurred much earlier ($t \leq 0.5$ h), impeding knockdown. This key role of excess uncomplexed lipid in mediating cellular internalization of siRNA at the plasma membrane level is quite different from the well-documented role of excess cationic lipid in improving gene delivery by neutralizing extracellularly interfering serum components (*14*, *15*). At an N:P of 2, the level of cellular association increased linearly at a rate of 25 ng/h between 0.5 and 3 h. Within the same time period, the rate decreased

2-fold as the N:P was doubled to 4. However, the initial rate ($0 \leq t \leq 0.5$ h) was higher at an N:P of 4 (91 vs 53, 70, and 60 ng/h at N:Ps of 0.5, 1, and 2, respectively).

The percent of total siRNA that became cell-associated (% dose) doubled as the N:P was doubled between 0.5 and 2 (Table 2). From an N:P of 2 to an N:P of 4, the % dose leveled off as did the % knockdown of VEGF protein. Interestingly, only a fraction of the dose (11% at an N:P of 1) was sufficient to almost completely inhibit protein production. This is equivalent to approximately 2×10^{12} siRNA molecules, or 7×10^6 copies per cell. For every protein molecule knocked down, there were ~2500 cell-associated siRNA molecules. To the best of our knowledge, this is the first time a correlation has been made between the amounts of cell-associated siRNA molecules and downregulated target protein molecules.

Particle Size and ζ Potential Measurements. Figure 5 shows particle sizes and ζ potentials of 1,3lb2−siRNA complexes. The lipoplexes were several hundred nanometers in diameter, ranging from 268 ± 4 nm at an N:P of 1 to 785 ± 62 nm at an N:P of 4. The low polydispersity index (PDI) values of the lipoplexes indicate fairly homogeneous particle size distributions. Only lipoplexes at an N:P of 4 had a positive ζ potential.

Interestingly, the particle sizes and ζ potentials at N:Ps of 0.5 and 1 were nearly identical, yet at an N:P of 0.5, there was no inhibition of VEGF production as opposed to 86% knockdown at an N:P of 1. The PDI at an N:P of 0.5 (0.34) was 1.5−2-fold higher than that of the other lipoplexes, and the greater heterogeneity of the particle size distribution at this N:P may have contributed to the lack of bioactivity. More likely, as mentioned in the previous section, the absence of knockdown was attributed to a deficiency in excess free lipid available to facilitate the membrane interaction necessary for cellular internalization of siRNA and/or its release into the cytosol.

Complexation Studies. Unlike pDNA, the much shorter and more rigid structure of siRNA (23 nucleotides vs several kilobases for pDNA) averts cationic lipid-induced compaction (*10*, *16*). Therefore, when EtBr-intercalated siRNA was titrated with 1,3lb2, the reduction in EtBr fluorescence emission intensity that was observed was not necessarily caused by the dye's displacement from the siRNA duplex. siRNA-bound lipid quenches the fluorescence of the intercalated dye; thus, the intensity decrease is an indication of binding and was used to calculate the complexation efficiency according to eq 2. Figure 6A shows the % binding as a function of N:P. The sigmoidal shape of the plot reflected positively cooperative binding; that is, the affinity of siRNA for 1,3lb2 increased as a function of lipid saturation. At an N:P of 0.5, there was only 20% interaction between 1,3lb2 and siRNA. Half the maximum binding was achieved at an N:P of ~1. Binding reached 94% at an N:P of 2, and extrapolation of the curve fit revealed complete binding around an N:P of 3.

Figure 6B shows the siRNA complexation efficiency of 1,3lb2 via agarose gel electrophoresis. At N:Ps from 0.25 to 2, the band intensity decreased by 2-fold as the N:P was doubled. At an N:P of 0.5, there was a 19% decrease in the intensity, and the level of reduction increased to 41% at an N:P of 1. The intensity was reduced by 82% at an N:P of 2 and was completely absent at an N:P of 3, signifying complete binding between 1,3lb2 and siRNA. These values match well with the corresponding binding percentages from the titration study.

Scatchard and Hill analyses (*17*) of the titration curve revealed a cooperative binding mechanism (Figure 6C). The concave-downward curve of the Scatchard plot was indicative of positive cooperativity which was also confirmed by a Hill slope value of 3. The Hill plot yielded a K_A of 1.17×10^5 M^{-1}, falling within the range of binding constants found in the literature for other cationic lipids (*18*, *19*).

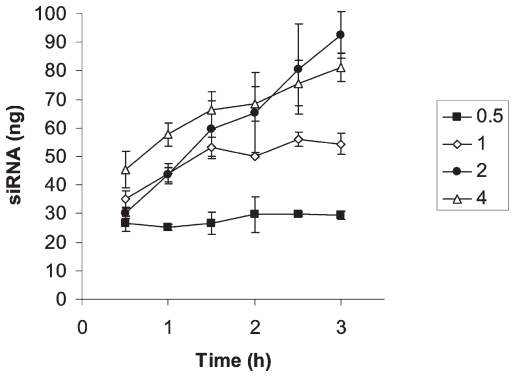

FIGURE 4: Change in the amount of cell-associated siRNA (mean ± standard deviation; $n = 2$) over time during siFection.

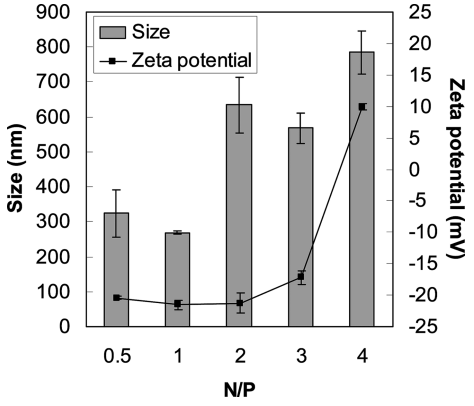

FIGURE 5: Particle size and ζ potential measurements of lipoplexes prepared at various N:Ps with 53.7 nM siRNA. The results are expressed as the mean ± the standard deviation ($n = 2$).

Table 2: Kinetic Parameters of Cell Association of siRNA in Lipoplexes at Various N:Ps

	rate of cellular association (ng/h)		cell-associated siRNA ($t = 3$ h)		
N:P	$0 \leq t \leq 0.5$ h	$0.5 \text{ h} \leq t \leq 3$ h	nanograms	% dose	% knockdown of VEGF protein[a]
0.5	52.8	0	29.4 ± 1.3	5.9 ± 0.3	0
1	70.3	18,[b] 0[c]	54.4 ± 3.8	10.9 ± 0.8	85.8 ± 4.1
2	60	24.5	92.6 ± 8.2	18.5 ± 1.6	94.4 ± 1.3
4	90.8	13.4	81.3 ± 5.0	16.3 ± 1.0	93.3 ± 1.1

[a]Values are from Figure 3A. [b]Between 0.5 and 1.5 h. [c]Between 1.5 and 3 h.

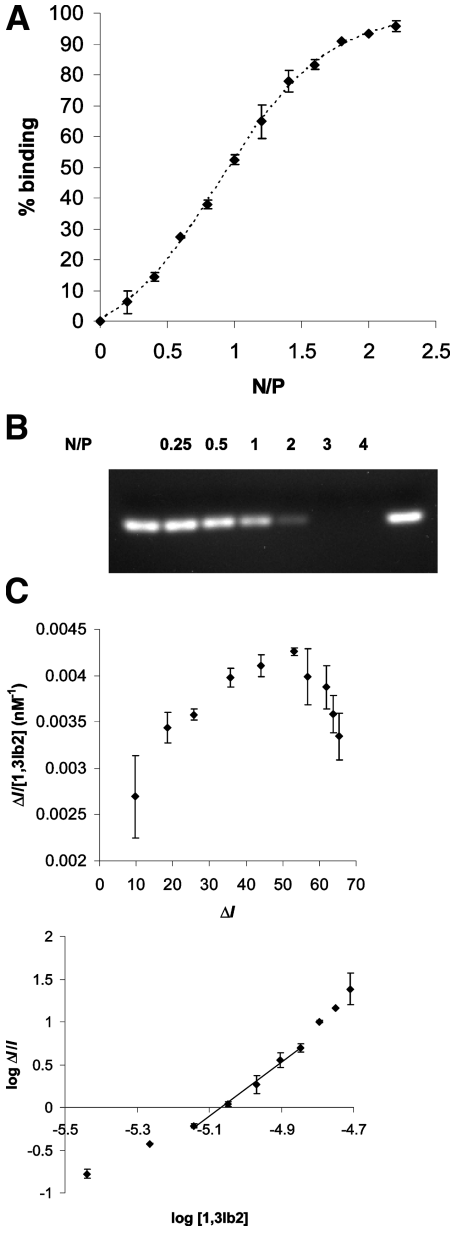

FIGURE 6: SiRNA complexation efficiency of 1,3lb2. (A) Plot of % binding (mean ± standard deviation; $n = 2$) between 1,3lb2 and siRNA as a function of N:P. The curve fit is represented by a dashed line. (B) Agarose gel electrophoresis of lipoplexes at N:Ps ranging from 0.25 to 4. Naked siRNA was loaded into the outermost wells. (C) Scatchard (top) and Hill (bottom) plots for the titration of a constant concentration of siRNA with 1,3lb2. The results are expressed as the mean ± the standard deviation ($n = 2$).

CONCLUSIONS

The optimized 1,3lb2 lipoplex formulation is a simple two-component system in which siRNA is completely bound to cationic lipid, as proven by the complexation studies. Further characterization of excess free lipid and of potentially "empty" liposomes, i.e., via separation of free lipid from siRNA-bound liposomes on a sucrose gradient (*20*, *21*), is not possible without disrupting the equilibrium of the system, a crucial balance between lipid monomers and lipoplexes.

The bioactivity of the 1,3lb2−VEGF-siRNA (phosphorothioate) complex was compared to those of other cationic vectors delivering native VEGF-siRNA reported in the literature (Table 3). To achieve a knockdown level of VEGF protein similar to that of 1,3lb2, a 4-fold increase in the N:P (from 2 to 8), a 2-fold increase in the siRNA concentration (from 53.7 to 100 nM), and a 3-fold increase in the concentration of cationic lipid (from 2.4 to 6.9 μM) were required for commercially available Lipofectamine (*6*). This corresponds to a 4-fold greater dose (1.49 μg vs 0.4 μg) and a 7.5-fold greater amount of cationic lipid (6 μg vs 0.8 μg) in the Lipofectamine formulation. The cationic component of Lipofectamine, DOSPA, is pentavalent, with a charge density 2.5-fold greater than that of 1,3lb2. Also, Lipofectamine contains an additional ingredient, the neutral colipid DOPE, which is not required for 1,3b2-mediated siFection. Optimized formulations of polyelectrolyte complexes (PECs), i.e., KALA- or PEI-PEGylated siRNA PECs, were found at N:Ps as high as 6 and 16, respectively, with as much as 200 nM siRNA (*22*). Kim et al. (*23*) reported a maximum of only 55% VEGF protein inhibition with 235 nM siRNA and 15 μM PECs containing a water-soluble lipopolymer (WSLP) of PEI when transfecting just 80000 cells (vs 300000 cells with 1,3lb2).

In summary, the cationic lipid 1,3lb2 was found to be a safe and efficacious cellular transporter of siRNA for potent knockdown of VEGF. It is a nontoxic delivery system that effectively binds siRNA and whose lipoplexes promote long-lasting inhibition, are highly bioactive at low N:Ps, and can function in the presence of serum. 1,3lb2 also has the potential for broader application, with the possibilities of successfully delivering other types of siRNA for silencing different targets as well as successful treatment in vivo in light of the high demand by the biopharmaceutical industry for proof of concept of RNAi-based therapeutics in primate subjects.

ACKNOWLEDGMENT

We thank Dr. Edward B. Dubrovsky (Department of Biological Sciences, Fordham University, Bronx, NY) for access to the Applied Biosystems 7300 Real-Time PCR System.

Table 3: Comparison of the 1,3lb2−VEGF-siRNA (phosphorothioate) Complex with Other Cationic Carriers of VEGF-siRNA (native)

			cationic agent		dose		lipid:siRNA ratio					
delivery system	no. of cells per well	no. of wells per plate	micromolar	micrograms	nanomolar	micrograms	N:P[a]	w/w	transfection time (h)	cell medium incubation time (h) prior to ELISA	% VEGF protein knockdown	ref
1,3lb2 dispersion	300000	12	2.4	0.8	53.7	0.4	2	2	3	48	94.4 ± 1.3	
Lipofectamine	200000	6[b]	6.9[b]	6[b]	100[b]	1.49[b]	8[b]	4	4	16	98.7	*6*
KALA PECs	200000	12	7.2[b]	NA[c]	200	NA[c]	6	NA[c]	4	18	90 ± 6.6	*22*
PEI PECs	200000	12	NA[c]	NA[c]	200	NA[c]	16	NA[c]	4	18	almost complete inhibition	*22*
WSLP PECs	80000	24	15[d]	7.35[b,d]	235[b]	1.05	NA[c]	7	4	16	55	*23*

[a]Nitrogen:phosphate ratio, except for 1,3lb2 (nitrogen:phosphorothioate ratio). [b]Calculated from available information. [c]Not available. [d]Value is with respect to the entire PEC, not the WSLP alone.

SUPPORTING INFORMATION AVAILABLE

Fluorescence emission scans of FITC-siRNA alone, in lipoplexes, and with both lipid and SDS (Figure S1), standard curve of FITC-siRNA fluorescence emission intensity (mean ± standard deviation) versus concentration (the solid line is the curve fit) (Figure S2), and plot of EtBr fluorescence emission intensity versus siRNA concentration (the solid line is the curve fit) (Figure S3). This material is available free of charge via the Internet at http://pubs.acs.org.

REFERENCES

1. Fire, A., Xu, S., Montgomery, M. K., Kostas, S. A., Driver, S. E., and Mello, C. C. (1998) Potent and specific genetic interference by double-stranded RNA in *Caenorhabditis elegans*. *Nature 391*, 806–811.
2. Elbashir, S. M., Harborth, J., Lendeckel, W., Yalcin, A., Weber, K., and Tuschl, T. (2001) Duplexes of 21-nucleotide RNAs mediate RNA interference in cultured mammalian cells. *Nature 411*, 494–498.
3. Tijsterman, M., Ketting, R. F., and Plasterk, R. H. (2002) The genetics of RNA silencing. *Annu. Rev. Genet. 36*, 489–519.
4. de Fougerolles, A., Vornlocher, H. P., Maraganore, J., and Lieberman, J. (2007) Interfering with disease: A progress report on siRNA-based therapeutics. *Nat. Rev. Drug Discovery 6*, 443–453.
5. Kim, D. H., and Rossi, J. J. (2007) Strategies for silencing human disease using RNA interference. *Nat. Rev. Genet. 8*, 173–184.
6. Takei, Y., Kadomatsu, K., Yuzawa, Y., Matsuo, S., and Muramatsu, T. (2004) A small interfering RNA targeting vascular endothelial growth factor as cancer therapeutics. *Cancer Res. 64*, 3365–3370.
7. Ferrara, N., and Henzel, W. J. (1989) Pituitary follicular cells secrete a novel heparin-binding growth factor specific for vascular endothelial cells. *Biochem. Biophys. Res. Commun. 161*, 851–858.
8. Kim, K. J., Li, B., Winer, J., Armanini, M., Gillett, N., Phillips, H. S., and Ferrara, N. (1993) Inhibition of vascular endothelial growth factor-induced angiogenesis suppresses tumour growth in vivo. *Nature 362*, 841–844.
9. Leung, D. W., Cachianes, G., Kuang, W. J., Goeddel, D. V., and Ferrara, N. (1989) Vascular endothelial growth factor is a secreted angiogenic mitogen. *Science 246*, 1306–1309.
10. Spagnou, S., Miller, A. D., and Keller, M. (2004) Lipidic carriers of siRNA: Differences in the formulation, cellular uptake, and delivery with plasmid DNA. *Biochemistry 43*, 13348–13356.
11. Spelios, M., Nedd, S., Matsunaga, N., and Savva, M. (2007) Effect of spacer attachment sites and pH-sensitive headgroup expansion on cationic lipid-mediated gene delivery of three novel myristoyl derivatives. *Biophys. Chem. 129*, 137–147.
12. Spelios, M., and Savva, M. (2008) Novel N,N′-diacyl-1,3-diaminopropyl-2-carbamoyl bivalent cationic lipids for gene delivery: Synthesis, in vitro transfection activity, and physicochemical characterization. *FEBS J. 275*, 148–162.
13. Boger, D. L., Fink, B. E., Brunette, S. R., Tse, W. C., and Hedrick, M. P. (2001) A simple, high-resolution method for establishing DNA binding affinity and sequence selectivity. *J. Am. Chem. Soc. 123*, 5878–5891.
14. Song, Y. K., and Liu, D. (1998) Free liposomes enhance the transfection activity of DNA/lipid complexes in vivo by intravenous administration. *Biochim. Biophys. Acta 1372*, 141–150.
15. Yang, J. P., and Huang, L. (1997) Overcoming the inhibitory effect of serum on lipofection by increasing the charge ratio of cationic liposome to DNA. *Gene Ther. 4*, 950–960.
16. Bolcato-Bellemin, A. L., Bonnet, M. E., Creusat, G., Erbacher, P., and Behr, J. P. (2007) Sticky overhangs enhance siRNA-mediated gene silencing. *Proc. Natl. Acad. Sci. U.S.A. 104*, 16050–16055.
17. Levitzki, A. (1980) Quantitative Aspects of Allosteric Mechanisms, Springer-Verlag, Berlin.
18. Keller, M., Jorgensen, M. R., Perouzel, E., and Miller, A. D. (2003) Thermodynamic aspects and biological profile of CDAN/DOPE and DC-Chol/DOPE lipoplexes. *Biochemistry 42*, 6067–6077.
19. Marty, R., N'soukpoé-Kossi, C. N., Charbonneau, D., Weinert, C. M., Kreplak, L., and Tajmir-Riahi, H. A. (2009) Structural analysis of DNA complexation with cationic lipids. *Nucleic Acids Res. 37*, 849–857.
20. de Jonge, J., Holtrop, M., Wilschut, J., and Huckriede, A. (2006) Reconstituted influenza virus envelopes as an efficient carrier system for cellular delivery of small-interfering RNAs. *Gene Ther. 13*, 400–411.
21. Nakamura, Y., Kogure, K., Futaki, S., and Harashima, H. (2007) Octaarginine-modified multifunctional envelope-type nano device for siRNA. *J. Controlled Release 119*, 360–367.
22. Lee, S. H., Kim, S. H., and Park, T. G. (2007) Intracellular siRNA delivery system using polyelectrolyte complex micelles prepared from VEGF siRNA-PEG conjugate and cationic fusogenic peptide. *Biochem. Biophys. Res. Commun. 357*, 511–516.
23. Kim, W. J., Chang, C. W., Lee, M., and Kim, S. W. (2007) Efficient siRNA delivery using water soluble lipopolymer for anti-angiogenic gene therapy. *J. Controlled Release 118*, 357–363.